

Clinical implications of convergent procoagulant toxicity and differential antivenom efficacy in Australian elapid snake venoms



Christina N. Zdenek^a, Bianca op den Brouw^a, Daniel Dashevsky^a, Alexandra Gloria^a, Nicholas J. Youngman^a, Ebony Watson^a, Patrick Green^a, Chris Hay^b, Nathan Dunstan^c, Luke Allen^c, Bryan G. Fry^{a,*}

^a Venom Evolution Lab, School of Biological Sciences, The University of Queensland, St. Lucia, QLD 4072, Australia

^b Australian School of Herpetology, Southport, QLD, Australia

^c Venom Supplies Pty Ltd, Stonewell Rd, Tanunda, SA, 5352, Australia

ARTICLE INFO

Keywords:

Venom
Venom-induced consumption coagulopathy
Coagulopathy
Antivenom
Venom evolution
Elapid

ABSTRACT

Australian elapid snakes are some of the most venomous snakes in the world and are unique among venomous snakes in having mutated forms of the blood clotting factor X in an activated form (FXa) as a key venom component. In human bite victims, an overdose of this activated clotting enzyme results in the systemic consumption of fibrinogen due to the large amounts of endogenous thrombin generated by the conversion of prothrombin to thrombin by venom FXa. Within Australian elapids, such procoagulant venom is currently known from the tiger snake clade (*Hoplocephalus*, *Notechis*, *Paroplocephalus*, and *Tropidechis* species), brown/taipan (*Oxyuranus* and *Pseudonaja* species) clade, and the red-bellied black snake *Pseudechis porphyriacus*. We used a STA-R Max coagulation analyser and TEG5000 thromboelastographs to test 47 Australian elapid venoms from 19 genera against human plasma in vitro. In addition to activity being confirmed in the two clades above, FXa-driven potent procoagulant activity was found in four additional genera (*Cryptophis*, *Demansia*, *Hemiaspis*, and *Suta*). Ontogenetic changes in procoagulant function was also identified as a feature of *Suta punctata* venom. Phylogenetic analysis of FX sequences confirmed that snake venom FXa toxins evolved only once, that the potency of these toxins against human plasma has increased in a stepwise fashion, and that multiple convergent amplifications of procoagulant activity within Australian elapid snakes have occurred. Cofactor dependence tests revealed all procoagulant venoms in our study, except those of the tiger snake clade, to be highly calcium-dependent, whereas phospholipid dependence was less of a feature but still displayed significant variation between venoms. Antivenom testing using CSL Tiger Snake Antivenom showed broad but differential cross-reactivity against procoagulant venoms, with *P. porphyriacus* and *S. punctata* extremely well neutralised but with *Cryptophis*, *Demansia*, and *Hemiaspis* less well-neutralised. The relative variation was not in accordance to genetic relatedness of the species used in antivenom production (*Notechis scutatus*), which underscores a fundamental principle that the rapid evolution characteristic of venoms results in organismal phylogeny being a poor predictor of antivenom efficacy. Our results have direct and immediate implications for the design of clinical management plans in the event of snakebite by such lesser known Australian elapid snake species that have been revealed in this study to be as potent as the better studied, and proven lethal, species.

1. Introduction

Snakebite is a globally neglected tropical disease which has recently been formally reclassified as such (WHO.int) and received US\$100 m from the Wellcome Trust to improve snakebite treatments (Schiermeier, 2019). Envenomings can cause permanent debilitation and death: up to 5.5 million people are bitten by snakes each year, around 300,000 of

which are left with debilitating morbidity and 94,000 of which prove fatal (Kasturiratne et al., 2008).

Effects upon blood coagulation are a major pathology produced by Australian venomous snakes in Elapidae. Activation of prothrombin into thrombin by these venoms results in consumptive coagulopathy, leading to disappearance of fibrinogen from the plasma (Gan et al., 2009; Gulati et al., 2013; Isbister, 2010; Isbister et al., 2008), which can

* Corresponding author at: School of Biological Sciences, Gehrmann Building #60, The University of Queensland, St. Lucia, QLD 4067, Australia.

E-mail address: bgfry@uq.edu.au (B.G. Fry).

<https://doi.org/10.1016/j.toxlet.2019.08.014>

Received 27 June 2019; Received in revised form 16 August 2019; Accepted 19 August 2019

Available online 20 August 2019

0378-4274/ © 2019 Elsevier B.V. All rights reserved.

be fatal if not arrested early enough (Sutherland and Tibballs, 2001). The quick consumption of the blood clotting factors prothrombin and fibrinogen renders the circulatory system unable to maintain haemostatic control, resulting in an increased tendency to bleed, with secondary effects including renal failure and cerebral haemorrhage (Sutherland and Tibballs, 2001; White, 2005). Once these clotting factors are consumed via activation of the blood coagulation cascade, protein synthesis of new factors by the body requires ~14 h (Isbister et al., 2009). While antivenom can prevent venom toxins from continuing to affect their molecular targets, it cannot reverse coagulotoxic effects once they occur because the activation of coagulation factors involves proteolysis (protein cleavage) which cannot be undone.

The pathophysiological effects produced by Australian elapid venoms upon the blood clotting cascade are due to the recruitment of the activated form (FXa) of the blood clotting factor X into the venom (FX) (Fry, 2005). FX is produced in the liver and circulates in the bloodstream in inactivated form (FX zymogen) until activated by either FIXa in the presence of FVIIIa from the intrinsic pathway, or FVIIa in the presence of tissue factor from the extrinsic pathway to create the active form, FXa (Greenberg and Davie, 2006). However, the form secreted in the venom glands of Australian elapids lack all or most of this activation peptide in its structure, and is therefore secreted in the activated form FXa (Trabi et al., 2015). Thus, snake venom FXa (SV-FXa) does not require proteolytic activation in order to exert a pathophysiological effect.

Sequences of mature of SV-FXa are around 80% identical to the FX expressed in the liver of the same species and share around 50% identity with the mammalian FX (Reza et al., 2006). Specific changes to the gene sequence have enabled SV-FXa to be an effective toxin. These changes include an insertion in the promoter region that leads to high expression levels in the venom gland as well as a shortened activation peptide region which allows the toxin to be active by default (Rao et al., 2004; Reza et al., 2005). SV-FXa also retains glycosylations similar to FX (Joseph et al., 1999), whereas the glycosylation is usually removed from the coagulation FXa (Trabi et al., 2015). The retention of the glycosylation in SV-FXa likely increases its stability and enables this compound to persist for longer in the bloodstream, since deglycosylated SV-FXa are rapidly destroyed by haemostasis regulatory enzymes (Reza et al., 2005; Trabi et al., 2015).

In the blood, the activated form of normal FX (FXa) associates with cofactors Factor Va (FVa), calcium, and phospholipid, to form the prothrombinase complex which converts prothrombin into thrombin; thrombin in turn cleaves fibrinogen (which is soluble in plasma) into insoluble fibrin strands that associate with platelets and red blood cells to create a haemostatic plug and arrest bleeding (Colman et al., 2006; Greenberg and Davie, 2006). In contrast to the dependency of endogenous FXa, significant variation in venom potency has been noted for venom FXa in the presence or absence of calcium and phospholipid (Lister et al., 2017; Zdenek et al., 2019).

Within the Australian elapids (Elapidae; subfamily: Hydrophiinae), the clade consisting of the genera *Hoplocephalus*, *Notechis*, *Paroplocephalus*, and *Tropidechis* require endogenous FVa from the bite victim as a cofactor to exert the full toxic effect, as the FXa toxin by itself is a poor activator of prothrombin (Gulati et al., 2013; Kini et al., 2002; Kwong and Kini, 2011). In contrast, in the *Oxyuranus* + *Pseudonaja* clade, FVa was additionally recruited into the venom as a toxin which forms a complex with SV-FXa (Fry, 2005), called FXa:FVa, thereby enabling prothrombin cleavage without requiring endogenous FVa or a phospholipid membrane from the bite victim's circulatory system on which to form the prothrombinase complex (Colman et al., 2006; Fry, 1999; Kwong and Kini, 2011; Tracy et al., 1982). This procoagulant complex makes up a large percentage of the total protein composition of these venoms: 10–20% of the total *O. scutellatus* venom (Lavin and Masci, 2009) and 16–20% of *P. textilis* venom (Rao and Kini, 2002). In contrast, FXa in both *N. scutatus* and *T. carinatus* venoms accounts for 5% of total venom composition (Kini, 2005). Thus, the

difference in coagulotoxin types and expression levels both likely account for the faster clotting times produced by venoms from the *Pseudonaja* + *Oxyuranus* clade (~5–10 s at 20 µg/ml venom) (Zdenek et al., 2019) compared to the tiger snake clade times (~9–15 s) (Lister et al., 2017).

A recent study revealed the tiger snake clade (*Hoplocephalus*, *Notechis*, *Paroplocephalus*, and *Tropidechis*) to have a high level of SV-FXa toxin sequence conservation (98.5% sequence alignment across the clade), coinciding with conserved cleavage sites on the FXa target, prothrombin (Lister et al., 2017). These results were corroborated by high levels of tiger snake antivenom efficacy across the clade (Lister et al., 2017), despite the divergence of these species being estimated to occur 6 million years ago (Lee et al., 2016).

Transcriptomic analyses have identified venom-expressed FXa in other Australian snakes, such as *Cryptophis nigrescens*, *Demansia* spp, *Hemiaspis* spp, *Pseudechis porphyriacus*, and *Suta suta* (Jackson et al., 2013; St Pierre et al., 2007). The functional activity of these toxins has not been tested; however, based on transcriptomic sequence similarity, it is expected that these SV-FXa toxins share a similar function to that previously described in the tiger snake clade (*Hoplocephalus*, *Notechis*, *Paroplocephalus*, and *Tropidechis*) and the *Oxyuranus* + *Pseudonaja* clade. This may explain, in part, why Tiger Snake Antivenom is able to cross-neutralise the symptoms of bites from some species beyond the tiger snake clade (Lane et al., 2011).

The coagulotoxic function of the venom from the most medically important species within Australia and the ability of antivenoms to neutralise this specific activity has only recently been investigated and described in detail (Lane et al., 2011; Lister et al., 2017; Zdenek et al., 2019). Less medically significant species are still largely unstudied in this regard, with one exception regarding the genus *Denisonia* (Youngman et al., 2018). Despite coagulopathy being a prominent pathology in snakebite victims within Australia, there has not been a broad comparison of coagulotoxic activity in the venom from species across the Australian elapids.

Which Australian snake venoms contain FXa and, if present, the relative efficacy of antivenom in neutralising these life-threatening effects is unknown. While the activated form of FX (FXa) was recruited for use as a toxin near the base of the Australian elapid radiation (Fry et al., 2008; Trabi et al., 2015), it has only been documented as being amplified in three clades: 1) *Hoplocephalus*, *Notechis*, *Paroplocephalus*, and *Tropidechis*; 2) *Oxyuranus* + *Pseudonaja*; and 3) *Pseudechis porphyriacus*. As these three clades are not sister to each other, and with a large number of other species intervening, it is likely that other lineages also possess this dangerous trait in their venoms and therefore are capable of producing similarly potent pathophysiological effects. The aim of this study was therefore to widely screen Australian snake venoms for the FXa-driven procoagulant coagulopathy and to ascertain the effectiveness of antivenom in neutralising these potentially lethal effects. As such, we conducted a broad assessment of Australian elapid venom effects on plasma and the efficacy of Tiger Snake Antivenom. We further investigated the evolution of SV-FXa toxins using cofactor dependence tests of calcium and phospholipid as well as sequence analyses.

2. Methods

2.1. Venom collection and preparation

We included 47 crude venoms across 19 clades within Elapidae sourced from the cryogenic collection of the Venom Evolution Lab. Only venoms from adult snakes were used so as to avoid the confounding variables such as of ontogenetic venom variation (e.g. Cipriani et al., 2017), excluding *S. punctata* for which an ontogenetic test was specifically conducted. Venoms were extracted using traditional (membrane) methods or via the pipette method (for low-yielding species) (Mirtschin et al., 2006). Upon extraction, all venoms were flash-

frozen in liquid nitrogen, lyophilised, and later reconstituted in deionised water, centrifuged (5 min., 4 °C, 14,000 RCF), and the supernatant was diluted to a concentration of 1 mg/ml with 50% glycerol and stored at –20 °C. Protein concentrations were determined in triplicate using a NanoDrop 2000 UV–Vis Spectrophotometer (ThermoFisher, Sydney, NSW, Australia) at an absorbance of 280 nm. Venoms were not pooled and were obtained from both wild-caught and captive-bred individuals. This is unlikely to influence our results; research on *Pseudonaja* indicates that captivity does not influence venom composition over time (McCleary et al., 2016), and only minor differences related to toxins present at low abundance in the venoms were observed in the majority of *Bothrops* snakes studied (Amazonas et al., 2019). All venom work was undertaken under University of Queensland Biosafety Approval #IBC134BSBS2015.

2.2. Plasma collection and preparation

Tests were undertaken using 3.2% sodium citrated human plasma, which was collected from healthy human donors and donated by the Australian Red Cross (Research Agreement #18-03QLD-09 and University of Queensland Human Ethics Committee Approval #2016000256). Once obtained, the plasma was thawed at 37 °C, aliquoted into 1.2 mL quantities, flash frozen in liquid nitrogen, and immediately stored at –80 °C until required. For phospholipid dependency tests, one pooled plasma bag (label #9521903 (O+)) was used. For all other tests, two pooled plasma bags (label #5251920 (O+) and label #4914041 (A+)) were combined before aliquoting and freezing at –80 °C until required. When required, plasma aliquots were rapidly thawed at 37 °C in a Thermo Haake ARCTIC immersion bath circulator (SC150-A40) and immediately used for experimentation. Plasma was replaced every hour at maximum during experimentation to maintain freshness.

2.3. STA-R Max assays

2.3.1. Coagulation

Coagulation tests were performed as previously described (Zdenek et al., 2019) using a STA-R Max® analyser (Stago, Asnières sur Seine, France). The time it took for the venom to cause human plasma to clot was measured automatically via a viscosity-based (mechanical) detection system involving opposing magnets and a small metal ball inside the test cuvette. Reagents included in each cuvette for each test were: phospholipid (Stago Cat# 00597), Owren Koller (OK) Buffer Stago Cat# 00360), CaCl₂ (25 mM, Stago Cat# 00367). Venom dilutions (0.05–20 µg/ml) for 8-point curves were automatically performed by the machine. Once venom and reagents were added to the cuvette, incubation for 120 s occurred at 37 °C, then plasma was added, and finally the time until clot formation was measured. Venom was replaced every 15–30 min to minimise enzymatic degradation. We tested the coagulotoxicity of 47 venoms from 42 elapid snake species across 19 genera within Australia. We included one non-Australian elapid species as an outgroup (*M. ikaheka*) and one positive control (Bovine FXa) for comparison.

2.3.2. Cofactor dependence tests

Cofactor dependence was assessed for 19 procoagulant species across 9 genera. To determine the level of cofactor dependence of the venoms, the aforementioned coagulation tests were conducted again at the highest venom concentration (20 µg/ml)—also in triplicate—with either calcium or phospholipid being replaced with OK Buffer to maintain consistent final volumes in the assay. Cofactor dependence values (x-fold shift in clotting times) were calculated by dividing the venom-without-cofactor clotting time by the venom-with-cofactor clotting time, then subtracting by one, whereby a shift of zero would indicate no shift. The machine maximum measuring time is 999 s, so if a test reached this time, an x-fold shift in clotting time was calculated

with the caveat that the measuring time was attenuated (at 999 s) and thus presented as ' $> X \pm SD$ '. These venoms were considered highly calcium dependent (HCD), and neither statistical analyses nor phylogenetic mapping of this trait were performed.

2.3.3. Antivenom efficacy

Antivenom efficacy was tested for 18 procoagulant species across 9 genera using IgG Monovalent Tiger Snake Antivenom (lot # 0550-09401; expiry 2003) from Commonwealth Serum Laboratories (CSL) Limited (Parkville 3052, Victoria). An examination of the activity of expired antivenoms demonstrated their effectiveness long past its expiry date and thus usefulness for research purposes (O'Leary et al., 2009). In addition, 58-year-old Tiger Snake Antivenom performed as well in coagulation assays on *N. scutatus* venom as did 14-year-old Tiger Snake Antivenom (Lister et al., 2017). Tiger Snake Antivenom is prepared from the plasma of horses immunised with the venom of *Notechis scutatus*.

For our assays, antivenom was centrifuged (using Allegra™ X-22R Centrifuge, Beckman Coulter, USA) at 14,000 RCF for 10 min at 4 °C. The supernatant fluid was filtered (0.45 µm Econofiltr PES, Agilent Technologies, China) and aliquoted into 2 ml Eppendorf tubes and stored at 4 °C until use. For testing, antivenom was diluted 1:20 in OK Buffer (ie. 5% antivenom/95% OK Buffer; 50 µl antivenom into 1000 µl total). The resulting final dilution of antivenom in the assay was 1:200 (1.25 µl antivenom in 250 µl total cuvette volume). Aforementioned coagulation tests performed on the STA-R Max® analyser were modified so that 25 µl of OK Buffer was replaced with 25 µl of the antivenom/OK buffer solution, thereby maintaining the final 250 µl test volume. To calculate antivenom efficacy, the AUC (Area Under the Curve) values for the venom + antivenom dose-response curves were divided by the venom-only dose-response curve AUC values, then subtracted by 1 so that no shift in AUC values (a value of 1 divided by 1) would have a value of 0 instead of 1.

2.3.4. Phylogenetic comparative analyses

The phylogenetic tree used was based upon a previously published species tree (Lee et al., 2016) and manually recreated using Mesquite software (version 3.2) and then imported to Rstudio using the APE package (Paradis et al., 2004). Ancestral states were estimated for all traits using maximum likelihood as implemented in the contMap function of the R package phytools (Revell, 2012). As in previous studies with these methods (Lister et al., 2017; Rogalski et al., 2017), we used the phytools script shown in Supplementary File 1.

2.4. Thromboelastography

To measure the strength of clots produced by the venoms, and the total thrombus generated, we employed thromboelastography. Clot strength assays were conducted as previously described by us (Oulion et al., 2018; Sousa et al., 2018). In brief, OK Buffer, calcium, phospholipid, venom, and finally plasma were added to the cup and pipette-mixed before measurements commenced on the Thromboelastograph® 5000 Haemostasis analyser (Haemonetics®, Haemonetics.com, Cat# 07-033) and proceeded for 30 min.

2.5. FXa-toxin molecular evolution

2.5.1. Phylogenetic reconstruction

Publicly available protein sequences for liver and venom gland expressed forms were retrieved from the UniProt database (Consortium, 2017). The sequences were aligned using a combination of manual alignment and the MULTIPLE Sequence Comparison by Log-Expectation (MUSCLE) algorithm implemented in AliView (Edgar, 2004; Larsson, 2014). We reconstructed the phylogeny of these sequences using MrBayes 3.2 for 15,000,000 generations and 1,000,000 generations of burnin with lset rates = invgamma (allows rate to vary with some sites

invariant and other drawn from a γ distribution) and preset aamodelpr = mixed (allows MrBayes to generate an appropriate amino acid substitution model by sampling from 10 predetermined models) (Ronquist et al., 2012). The run was stopped when convergence values reached 0.01. The sequence alignment used in these analyses is shown in Supplementary File 2.

2.5.2. Tests for selection

Coding DNA sequences of venom gland expressed forms of FX were compiled from GenBank (Consortium, 2017). The sequences were trimmed to only include those codons which translate to the mature protein, and subsequently translated, aligned, and reverse translated using AliView and the MUSCLE algorithm (Edgar, 2004; Larsson, 2014). The phylogenetic tree generated earlier was used for the subsequent analyses.

We used several of the tests for selection implemented in HyPhy version 2.220150316beta due to their different emphases (Pond et al., 2005). The Analyze Codon Data analysis calculates the overall dN/dS ratio for an alignment. The Fast Unconstrained Bayesian Approximation (FUBAR) method gauges the strength of consistent positive or negative selection on individual amino acids (Murrell et al., 2013); in contrast, the Mixed Effects Model of Evolution (MEME) method identifies individual sites that were subject to episodes of positive selection in the past (Murrell et al., 2012).

2.5.3. Protein modelling

A custom model for the toxin form of Factor X was generated by inputting a representative sequence into the Phyre2 webserver using the Intensive option (Kelley et al., 2015). Attribute files were created from FUBAR and MEME results and these were used to colour the Phyre2 structure in UCSF Chimera version 1.10.2 (Pettersen et al., 2004).

3. Results

3.1. STA-R Max assays

3.1.1. Coagulation

Ancestral state reconstruction of clotting times produced by venoms at 20 $\mu\text{g}/\text{ml}$ on pooled human plasma is shown in Fig. 1. Venoms which clotted plasma within 0–200 s were considered procoagulant in that they promoted clot formation relative to the spontaneous clotting time of recalcified healthy plasma in the absence of venom (negative control): 420.3 ± 68.7 s. Mapping values over the tree revealed that the tiger snake clade (Lister et al., 2017) and *Pseudonaja* + *Oxyuranus* (Zdenek et al., 2019) were strongly procoagulant, and *Pseudonaja textilis* produced the fastest clotting time (~5 s) of any venom tested. Four additional genera (*Cryptophis*, *Demansia*, *Hemiaspis*, and *Suta*) were found to contain species whose venoms were notably procoagulant. Plasma clotting times produced by *Suta* spp. venoms varied widely and an ontogenetic shift in *Suta punctata* was noted. Adult *S. punctata* rapidly clotted plasma (at 20 $\mu\text{g}/\text{ml}$ a clotting time of 15.3 ± 0.1 s, with an area under the curve of 384.3 ± 2.08) while *S. punctata* juvenile venom was much less potent (at 20 $\mu\text{g}/\text{ml}$ a clotting time of 34.2 ± 0.2 s, with an area under the curve of 887.2 ± 2.11). The next most potent *Suta* species, *S. spectabilis*, was significantly less potent (at 20 $\mu\text{g}/\text{ml}$ 129.7 ± 9.4 s), and *S. fasciata* was even less potent (250.9 ± 13.5 s). All other *Suta* species did not show evidence of procoagulant activity. Thus there is significant interspecies variation within the *Suta* genus in addition to the significant ontogenetic variation for *S. punctata*.

All sea snake (*Hydrophis* spp. and *Aipysurus laevis*) venoms showed no activity on plasma, with clotting times within or near the negative control range. Venoms which clotted plasma within 800–999 s were considered anticoagulant in that they delayed or prevented clot formation relative to the negative control range of 420.3 ± 68.7 s. Four

venoms (*A. antarcticus*, and *D. devisii*, *D. maculata*, and *P. australis*) were found to be anticoagulant.

3.1.2. Cofactor dependence

The FXa positive control and all procoagulant venoms, except for those of the tiger snake clade, were found to be highly calcium dependent, with the machine maximum time (999 s) being reached for all venoms without calcium in the assay (Table 2). Endogenous FXa was also highly calcium dependent, indicating this feature is the ancestral state. Thus, the dramatically reduced dependence on calcium in the tiger snake clade, and the *Oxyuranus* + *Pseudonaja* clade represent two convergent molecular adaptations for lessened biochemical dependence upon calcium. Overall, the removal of calcium produced much greater effects on venom action than did removing phospholipid. We observed extensive variation in phospholipid dependence (Table 2) but with little correlation relative to calcium dependence. Such dichotomy has been observed for other lineages such as *Echis* (Rogalski et al., 2017) while in contrast a correlation between calcium and phospholipid dependency patterns has been observed in other lineages (Lister et al., 2017; Zdenek et al., 2019).

3.1.3. Antivenom efficacy

While the tiger snake antivenom displayed cross-reactivity against all the procoagulant venoms, there was significant differential efficacy. The tiger snake clade (*Hoplocephalus*, *Notechis*, *Paroplocephalus*, and *Tropidechis*) (Lister et al., 2017) and also *P. porphyriacus* (Figs. 2 and 3) were extremely well neutralised. In contrast, the *Cryptophis*, *Demansia* and *Hemiaspis* venoms were not as well neutralised. There was no phylogenetic association, as the two most poorly neutralised genera represented the closest (*Hemiaspis*) and the most divergent (*Demansia*) relative to the tiger-snake clade, a member of which (*N. scutatus*) was the only venom used in the immunising mixture during Tiger Snake Antivenom production and the only FXa rich venom used in the production of Australian Polyvalent Antivenom. Similarly, *P. porphyriacus* was extremely well neutralised despite being phylogenetically distinct from *N. scutatus*.

3.2. Thromboelastography assays

Representatives of each procoagulant genus were tested by thromboelastography to ascertain if strong, stable clots were being formed consistent with the generation of endogenous thrombin by FXa-driven procoagulation. Indeed all venoms produced clots with maximum amplitude (MA) and total thrombus generation (TGG) values similar to that of the three control tests (spontaneous clotting, FXa induced clotting, and thrombin induced clotting) (Fig. 2, Table 1). Indicative of their extreme potency, all venoms had speed of actions similar to that of the FXa and thrombin controls, as measured by split point (SP), time to reach 2 mm amplitude (R), maximum rate of thrombus generation (MRTG) and time to maximum rate of thrombus generation (TMRTG) (Fig. 2, Table 1). *D. vestigiata* was the only exception in this regard, having SP, R, MRTG, and TMRTG values that were markedly slower than all other venoms and the FXa and thrombin control enzymes, which was also consistent with the clotting time differences noted between *Demansia* and other procoagulant venoms in the STA-R Max tests (Fig. 1). However, consistent with the generation of endogenous thrombin and the production of strong stable fibrin clots, *D. vestigiata* was still significantly faster in all values relative to the spontaneous control and despite the slower action, *D. vestigiata* venom was comparable to that of other venoms and the controls in the strength of the clots ultimately formed, as indicated by the MA and TGG values produced by the venoms (Fig. 2, Table 1).

3.3. FXa-toxin molecular evolution

The phylogeny of the venom gland FXa forms was consistent with a

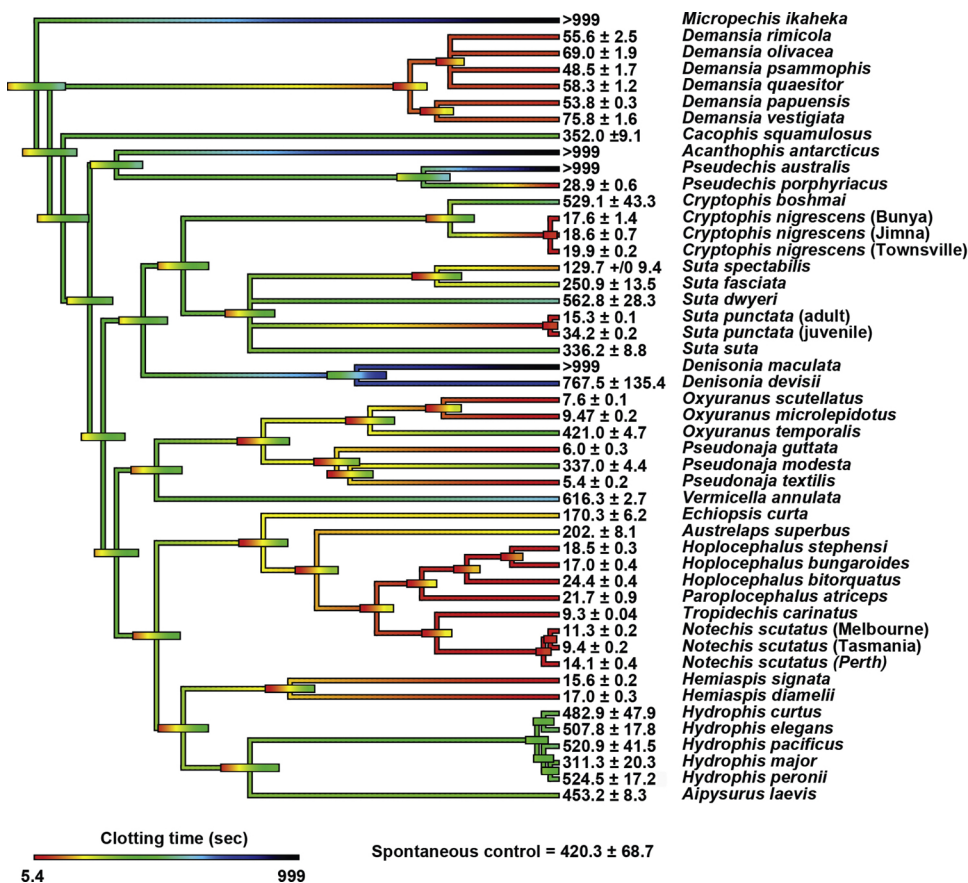


Fig. 1. Ancestral state reconstruction of clotting times (s) produced by venoms (20 µg/ml) on pooled human plasma, where warmer colours represent faster clotting times. Bars indicate 95% confidence intervals for the estimate at each node. Note: due to the dynamic nature of venoms, the bars rapidly become broad as one moves down the tree. Values are $N = 3$ mean ± SD.

single early recruitment event into the biochemical arsenal of the common ancestor of the Australo-Papuan elapids (Fry, 2005), with additional gene duplication and diversification in descendent lineages (Fig. 5). The venom gland FXa sequences formed two large clades, one that included the derived form (FXa:FVa) unique to the *Oxyuranus* + *Pseudonaja* clade, and a second clade that included toxins from all the other Australian elapid species. The tiger snake clade was contained within the latter and is known to have extremely conserved SV-FXa sequences (Lister et al., 2017), which can be a sign of negative selection. Despite this, our results show that the larger FXa-only clade is subject to positive selection overall with a calculated dN/dS ratio of 2.15, which is consistent with the differential cofactor dependence between the venoms. The results of our site-specific analyses are congruent with these findings: FUBAR determined that 49 sites show statistically significant signs of positive selection while MEME reported 10 such sites, 8 of which had also been detected by FUBAR. Consistent with a slower mode of action, and being the most phylogenetically basal snake genus demonstrating procoagulant action, *Demansia* sequences had only partially truncated activation peptides (Fig. 6 alignment positions 195–223). In alignment positions 326–338, insertions are present in the venom sequences relative to the endogenous liver-secreted form (Fig. 6). While the lack of this insertion in *Demansia* is consistent with this genus being slower in action, and suggestive of the insertion evolving after the divergence by this genus, the insertion was also lacking in the more derived *P. porphyriacus*, resulting from a secondary loss within this species. The functional impact of these insertions is unknown but does not display any correlation with relative dependence on calcium or phospholipid (Table 2). However, the lack of pattern between insertion sites and antivenom efficacy indicates that the antivenom efficacy is not due to binding at these sites. Similarly the lack of a phylogenetic signal between cofactor dependence and antivenom efficacy indicates that antivenom binding is to sites distinct from those involved in relative cofactor dependence.

4. Discussion

Our results revealed that more Australian elapid venoms are potentially procoagulant than previously recognised and that, while Tiger Snake Antivenom is broadly cross-reactive, it varies extensively in relative efficacy and therefore may have limited clinical usefulness or more antivenom may be required to neutralise the same amount of venom between species. Species in the *Cryptophis*, *Hemiaspis*, and *Suta* genera displayed levels of potency within the range shown previously for proven lethal species such as *N. scutatus* (Lister et al., 2017). While bites from *Cryptophis*, *Hemiaspis*, and *Suta* species are rare due to their remote ranges or nocturnal behaviour, the results in this study strongly suggest that envenomations may produce severe coagulopathy. The *Demansia* genus represents another undescribed procoagulant genus. While of lesser potency, *Demansia* species are capable of very large venom yields and thus may be able to produce clinically significant procoagulant envenomations. The antivenom performed extremely well on *P. porphyriacus* and *S. punctata* venoms, but with much lower efficacy against *Cryptophis*, *Demansia* and *Hemiaspis* venoms. The poor performance on *Hemiaspis* was particularly notable due to the close genetic relationship between this genus and *N. scutatus* from the tiger snake clade which was used in the antivenom production immunising mixture.

The results of this study indicate that, while FXa was recruited for use as a toxin at the base of the Australo-Papuan elapid snake radiation, it was secondarily amplified on seven independent occasions: 1) the *Demansia* genus; 2) *Pseudechis porphyriacus* as a unique derivation within the *Pseudechis* genus; 3) *Cryptophis* genus; 4) *Suta punctata* as a unique derivation within the *Suta* genus; 5) the *Oxyuranus* and *Pseudonaja* last common ancestor; 6) the *Hoplocephalus*, *Notechis*, *Paroplocephalus*, and *Tropidechis* last common ancestor; and 7) the *Hemiaspis* genus (Fig. 1). While *Hemiaspis* is closely related to the *Hoplocephalus*, *Notechis*, *Paroplocephalus*, and *Tropidechis* clade, it appears

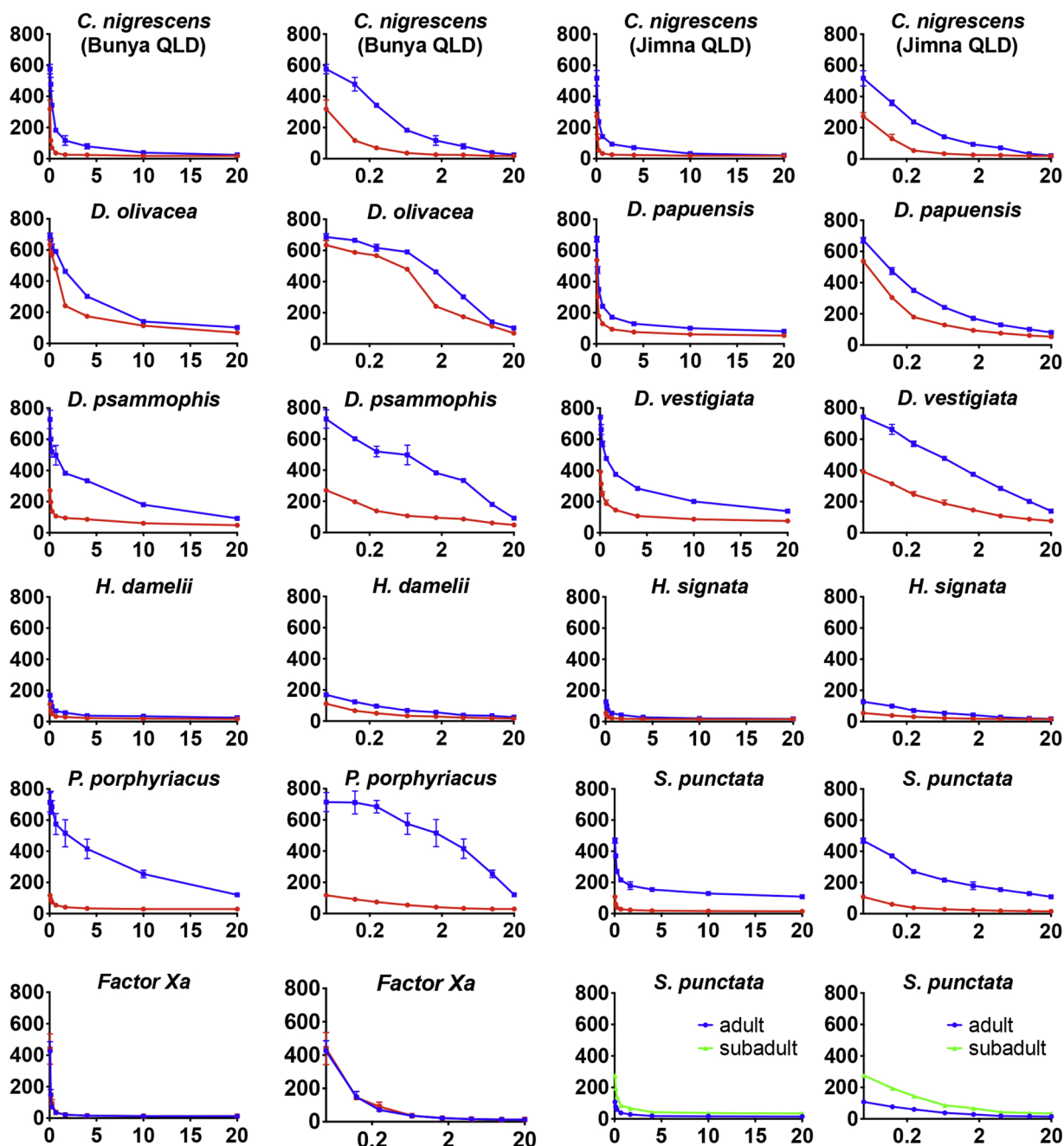


Fig. 2. Eight-point dilution curves, showing clotting times (y-axis; seconds) of human plasma combined with varying concentrations of venom (x-axis; $\mu\text{g}/\text{mL}$) presented in linear (left) and logarithmic views (right) for each species. Venom curves are shown in red and venom + antivenom curves are shown in blue. CSL Tiger Snake Antivenom was used at 0.5% in the assay. The last pair shows the ontogenetic variation between *S. punctata* adult and subadult venoms. Data points are $N = 3 \pm \text{SD}$. Note: for most data points the error bars are smaller than the datapoint symbols.

to represent an independent amplification of SV-FXa relative to the tiger snake clade, as a proteomic and transcriptomic analysis of *Drysdalia coronoides*—sister to the tiger snake clade—revealed a lack of SV-FXa amplification in its venom (Chatrath et al., 2010). The *Suta* genus was notable in that plasma clotting varied widely ontogenetically and between species. *Suta punctata* rapidly clotted plasma (15.3 ± 0.1 s, with an area under the curve of 384.3 ± 2.08) and over twice as quickly as *S. punctata* juvenile venom (34.2 ± 0.2 s, with an area under the curve of 887.2 ± 2.11), and other *Suta* spp. did not produce appreciable effects on plasma, with the exception of *S. fasciata* and *S. spectabilis* which produced moderate effects (Fig. 1).

Despite the extreme divergence of the snake species included in this study (~25 million years) (Lee et al., 2016), we demonstrated a

remarkably broad cross-reactivity of Tiger Snake Antivenom that was decoupled from relative phylogenetic affinities (Figs. 2 and 3). This unparalleled level of cross-reactivity is consistent with the overall extreme conservation of the SV-FXa toxins. However, there were variations, such as *Cryptophis*, *Demansia* and *Hemiaspis* being the least neutralised, which is indicative of variations in the surface chemistry of the toxins influencing relative epitope-paratope interactions. These variations are not the result of simple drift, as *Hemiaspis* is more related to the clade which contains the species (*N. scutatus*) used in the antivenom immunising mixture than is the more well-neutralised *P. porphyriacus* (Fig. 3). Therefore, the variation in antivenom neutralisation is indicative of the toxins evolving under positive selection pressure, which is also consistent with the results that showed that some surface sites

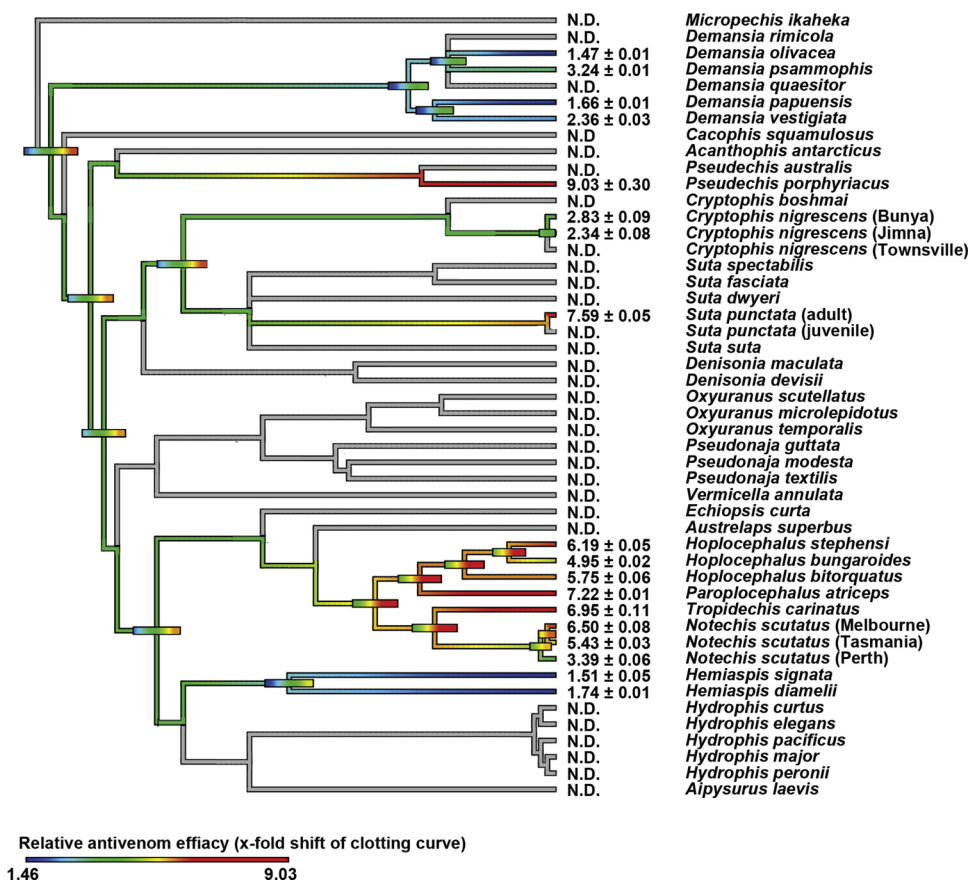


Fig. 3. Ancestral state reconstruction of anti-venom efficacy (x-fold shift of clotting curve AUCs with and without the addition of anti-venom) of procoagulant venoms (20 µg/ml) on pooled human plasma, where warmer colours represent faster clotting times. A value of zero would indicate no shift. Bars indicate 95% confidence intervals for the estimate at each node. Note: due to the dynamic nature of venoms, the bars rapidly become broad as one moves down the tree. Values are N = 3 mean ± SD. ND = not determined for lineages in gray due to being FXa-rich venoms for which sufficient stock was not available (*C. nigrescens* (Townsville), *D. quaesitor*, *D. rimicola*, and *S. punctata* (juvenile)), or venoms which were not relevant to Tiger Snake Antivenom due to being either FXa:FVa rich venoms (*Oxyuranus* and *Pseudonaja*) or not procoagulant (all others).

were episodically evolving under positive selection pressure (Fig. 4).

The specificity of the antivenom for certain surface structural features specific for venom FXa was underscored by its lack of cross-reactivity with endogenous human FXa (Fig. 3). As has been shown in other species, subtle variations in surface chemistry can have profound impacts upon antivenom specificity and efficacy and therefore high level of sequence similarity is a poor predictor of antivenom efficacy (Zdenek, et al., 2019). However, in other cases highly similar toxins were well neutralised, such as the extremely conserved FXa toxins with the *Hoplocephalus*, *Notechis*, *Paroplocephalus*, and *Tropidechis* clades resulting in very strong antivenom cross reactivity (Lister et al., 2017). In

contrast, a very poor level of antivenom cross reactivity has been shown in other clades, despite the toxins being highly conserved, such as the FXa:FVa coagulotoxin complex that evolved in the common ancestor of *Oxyuranus* and *Pseudonaja* (93% similarity of the FXa subunits and 97% similarity of the FVa subunits) (Zdenek et al., 2019). The results were surprising in that the antivenom developed using just *Oxyuranus* venom in the immunisation mixture failed to effectively neutralise the venoms from its sister genus *Pseudonaja*, despite the high level of sequence similarity between toxins from the two sister-genera (Zdenek et al., 2019). Thus, slight variations on the surface of the toxins can have dramatic effects both on toxin specificity and potency, in addition to

Table 1

Thromboelastography output values for traces produced by venoms (20 µg/ml) on human plasma, in the presence of cofactors, as per the Methods. Data are N = 3 means ± SD values.

| Species | MA (mm) | SP (min) | R (min) | MRTG (dcs, dynes/cm ² /s) | TMRTG (min) | TGG (dynes/cm ²) |
|----------------------------------|--------------|------------|------------|--------------------------------------|-------------|------------------------------|
| Negative control | 11.93 ± 1.76 | 16.3 ± 1.4 | 18.2 ± 1.7 | 1.0 ± 0.1 | 18.8 ± 0.7 | 79.7 ± 11.6 |
| Thrombin control | 13.23 ± 1.24 | 0.3 ± 0.1 | 0.5 ± 0.1 | 3.0 ± 0.2 | 0.9 ± 0.1 | 82.1 ± 9.6 |
| Bovine FXa control | 14.87 ± 1.05 | 0.8 ± 0.1 | 1.0 ± 0.1 | 3.9 ± 0.3 | 1.5 ± 0.1 | 95.0 ± 8.3 |
| <i>Cryptophis nigrescens</i> | 13.00 ± 0.36 | 0.5 ± 0.2 | 0.6 ± 0.2 | 4.7 ± 0.1 | 1.1 ± 0.2 | 81.0 ± 3.1 |
| <i>Demansia vestigiata</i> | 13.17 ± 0.98 | 5.0 ± 0.9 | 5.7 ± 0.9 | 2.9 ± 0.2 | 6.4 ± 0.8 | 76.4 ± 5.8 |
| <i>Hemiaspis signata</i> | 11.43 ± 1.18 | 0.4 ± 0.1 | 0.5 ± 0.1 | 5.1 ± 0.6 | 1.0 ± 0.1 | 62.3 ± 8.0 |
| <i>Hoplocephalus bungaroides</i> | 12.03 ± 1.20 | 0.2 ± 0.0 | 0.2 ± 0.1 | 5.3 ± 0.2 | 0.6 ± 0.2 | 63.1 ± 7.3 |
| <i>Notechis scutatus</i> | 13.30 ± 1.73 | 0.2 ± 0.0 | 0.2 ± 0.0 | 7.9 ± 1.8 | 0.3 ± 0.0 | 79.9 ± 12.4 |
| <i>Paroplocephalus atriceps</i> | 10.80 ± 1.05 | 0.4 ± 0.1 | 0.5 ± 0.1 | 4.6 ± 0.5 | 1.0 ± 0.1 | 61.0 ± 5.8 |
| <i>Pseudechis porphyriacus</i> | 12.47 ± 0.75 | 0.7 ± 0.1 | 0.9 ± 0.1 | 4.8 ± 0.4 | 1.3 ± 0.2 | 80.3 ± 5.5 |
| <i>Suta punctata</i> | 12.40 ± 1.04 | 0.5 ± 0.1 | 0.7 ± 0.1 | 4.3 ± 0.7 | 1.2 ± 0.1 | 75.5 ± 2.2 |
| <i>Tropidechis carinatus</i> | 12.90 ± 1.61 | 0.2 ± 0.0 | 0.2 ± 0.1 | 6.2 ± 1.5 | 0.5 ± 0.3 | 81.4 ± 10.3 |
| <i>Oxyuranus scutellatus</i> | 15.10 ± 1.37 | 0.2 ± 0.0 | 0.3 ± 0.1 | 5.1 ± 0.7 | 0.8 ± 0.1 | 94.3 ± 10.9 |
| <i>Pseudonaja textilis</i> | 15.10 ± 1.18 | 0.2 ± 0.0 | 0.2 ± 0.0 | 7.3 ± 0.8 | 0.3 ± 0.0 | 94.6 ± 7.2 |

MA = maximum amplitude; SP = split point; R = time to reach 2 mm amplitude; MRTG = maximum rate of thrombus generation (dcs, dynes/cm²/s). TMRTG = time to maximum rate of thrombus generation (min). TGG = total thrombus generation (dynes/cm²).

Table 2

Cofactor dependence, measured by x-fold shift of clotting times (s) with and without cofactors calcium or phospholipid (PPL), of procoagulant venoms. Bovine FXa was tested as a positive control. Higher x-fold shift indicates greater cofactor-dependence, and no shift is indicated by a value of 0. Values are N = 3 mean ± SD.

| Sample | clotting time (s) with calcium and PPL | x-fold shift without calcium (calcium dependence) [*] | x-fold shift without PPL (PPL dependence) |
|---|--|--|---|
| Factor Xa control | 12.2 ± 0.4 | > 81.2 ± 2.9 | 1.5 ± 0.1 |
| <i>Cryptophis nigrescens</i> (Bunya Mtns) | 14.7 ± 0.3 | > 56.1 ± 4.4 | 1.1 ± 0.0 |
| <i>Cryptophis nigrescens</i> (Jimna) | 16.0 ± 0.1 | > 61.3 ± 0.5 | 1.1 ± 0.0 |
| <i>Cryptophis nigrescens</i> (Townsville) | 15.9 ± 0.4 | > 61.9 ± 1.7 | 1.3 ± 0.1 |
| <i>Demansia papuensis</i> | 66.1 ± 1.0 | > 17.5 ± 0.1 | 1.5 ± 0.0 |
| <i>Demansia psammophis</i> | 56.1 ± 0.8 | > 19.6 ± 0.8 | 2.7 ± 0.1 |
| <i>Demansia vestigiata</i> | 99.8 ± 8.8 | > 12.2 ± 0.3 | 1.3 ± 0.0 |
| <i>Hemiaspis damelii</i> | 17.0 ± 0.3 | > 57.8 ± 0.7 | 2.8 ± 0.0 |
| <i>Hemiaspis signata</i> | 15.6 ± 0.2 | > 63.2 ± 0.6 | 2.1 ± 0.0 |
| <i>Hoplocephalus bitorquatus</i> | 24.4 ± 24.4 | 7.3 ± 0.3 | 1.4 ± 0.1 |
| <i>Hoplocephalus bungaroides</i> | 17.0 ± 0.4 | 8.0 ± 0.3 | 1.1 ± 0.1 |
| <i>Hoplocephalus stephensi</i> | 18.5 ± 0.3 | 6.5 ± 0.4 | 1.2 ± 0.2 |
| <i>Notechis scutatus</i> (Melbourne) | 11.3 ± 0.2 | 7.1 ± 0.2 | 0.9 ± 0.0 |
| <i>Notechis scutatus</i> (Perth) | 14.1 ± 0.4 | 6.2 ± 0.1 | 0.6 ± 0.0 |
| <i>Notechis scutatus</i> (Tasmania) | 9.4 ± 0.2 | 6.1 ± 0.1 | 0.6 ± 0.1 |
| <i>Paroplocephalus atriceps</i> | 21.7 ± 0.9 | 13.0 ± 0.6 | 1.2 ± 0.1 |
| <i>Pseudechis porphyriacus</i> | 28.9 ± 0.6 | > 33.5 ± 0.6 | 2.0 ± 0.2 |
| <i>Suta punctata</i> (adult) | 15.3 ± 0.1 | > 64.2 ± 0.4 | 6.8 ± 0.3 |
| <i>Suta punctata</i> (juvenile) | 34.2 ± 0.2 | > 28.2 ± 0.2 | 1.6 ± 0.0 |
| <i>Tropidechis carinatus</i> | 9.3 ± 0.04 | 10.4 ± 0.3 | 0.6 ± 0.1 |

* For venoms which reached the machine maximum measuring time (999 s) in the absence of calcium, the x-fold shift was calculated with the caveat that the measuring time was attenuated (at the 999 s mark), hence the '>' prior to the values. These venoms were considered highly calcium dependent (HCD).

relative antivenom efficacy. There was no phylogenetic pattern of antivenom efficacy (Fig. 3) regarding cofactor dependence (Table 2) or sequence insertions (Fig. 6). Therefore, the variation in antivenom efficacy was likely due to divergence on other sites on the enzyme molecular surface.

Along with several species that are now restricted to Papua New Guinea, *Demansia* is one of the most basal lineages of the elapid subfamily Hydrophiinae (Lee et al., 2016; Sanders et al., 2008; Strickland et al., 2016). However, the most basal split amongst the SV-FXa toxins in our toxin phylogenetic analysis was between the *Pseudonaja* + *Oxyuranus* clade and all others (Fig. 5). This discrepancy is likely due to the phylogenetic analyses failing to accurately capture the phylogenetic signal represented by the series of deletions in the activation peptide region of the venom FXa sequences: compared to the liver-expressed FX, *Demansia vestigiata* SV-FXa has a 10 amino acid deletion while those from more derived hydrophiines have a further 19 amino acids deleted (Fig. 6). This shows a clear pattern of stepwise evolution and, since gaps are not counted as mismatches in MrBayes, explains the incongruence between the phylogeny of the toxins and that of the species to which they belong. This evolutionary series of deletions may also explain the less potent coagulotoxicity we observed from *Demansia* spp. venoms; while no SV-FXa sequence has deleted the full extent of the activation peptide that is cleaved to form the liver-expressed FXa the larger deletion found in derived hydrophiines is significantly more similar than that of basal hydrophiines and may well enable these toxins to mimic the physiological role of FXa more effectively. Therefore, the sequences with more deleted amino acids in the activation peptide motif display the fastest clotting times. However, as with cofactor dependence or sequence insertions, there was no phylogenetic pattern of antivenom efficacy (Fig. 3) with regards to deletions of activation peptide amino acids (Fig. 6). This suggests the variation in antivenom efficacy was due to divergence on other sites on the enzyme molecular surface.

Between this refinement of venom FXa and the accompanying recruitment of a FVa equivalent in the *Pseudonaja* + *Oxyuranus* clade, it is clear that some lineages of hydrophiines have followed an evolutionary path towards stronger coagulotoxicity. This path is consistent with our signal of selection analyses that indicate that the FXa toxins are subject to net positive selection. This is the case for many other reptile toxin

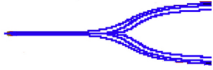
families (Brust et al., 2012; Dashevsky and Fry, 2018; Jiang et al., 2011; Juárez et al., 2008; Rokyta et al., 2011), but the snake venom form of FXa is unusual in its relatively high sequence conservation. It has been previously hypothesised that this unusual level of sequence conservation is due to a selection pressure exerted by the extremely conserved target (Lister et al., 2017). Variation in key sites involved in substrate recognition and cleavage would deleteriously affect the ability to exert the pathophysiological action and therefore such mutations would be under negative selection pressure. This is consistent with the theory put forth that globular venom components are under structural constraints that limit their diversification (Fry, 2005). However, while these toxins are largely conserved, those mutations which are apparent in the FX sequences available are skewed towards non-synonymous changes on the molecular surface which is evidence for at least some regions of these toxins being subject to diversifying selection for potency or specificity.

The variances in coagulotoxic potency observed across the procoagulant venoms in this study may be explained by one of two scenarios (or a combination thereof). One scenario may be that the venom expression levels of FXa differ across species. Alternatively, variation in the sequence of the toxins may lead to variable speed of action in which each individual toxin possesses in cleaving prothrombin to thrombin, either through variations in binding affinity or cleavage rate-of-action (or a combination of these two variables). There was not, however, a correlation between relative dependence on calcium or phospholipid cofactors and relative speed of action (Figs. 1 and 2, Table 1). This is in contrast to other venoms, such as from *Oxyuranus* and *Pseudonaja*, in which cofactor dependence was shown to be a driving variable in speed of action (Zdenek et al., 2019). However, the disconnect between cofactor variance and speed of action has been noted in the venom of some species, such as those within the genus *Echis* (Rogalski et al., 2017). It is notable, however, that a sharp decrease in the relative dependence upon calcium has evolved twice within the Australian elapid snake venoms: once in the last common ancestor of *Hoplocephalus*, *Notechis*, *Paroplocephalus*, and *Tropidechis*, with a further reduction in *Notechis* (Lister et al., 2017), and again independently in the *Oxyuranus* + *Pseudonaja* clade. As the relative dependence on calcium was not correlated with clotting time, unlike in the *Oxyuranus* + *Pseudonaja*

CONTROLS

Spontaneous clotting control

SP = 16.3 +/- 1.4 MRTG = 1.0 +/- 0.1
R = 18.2 +/- 1.7 TMRTG = 18.8 +/- 0.7
MA = 11.9 +/- 1.8 TGG = 79.7 +/- 11.6



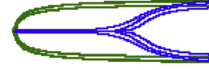
Factor Xa control

SP = 0.8 +/- 0.1 MRTG = 3.9 +/- 0.3
R = 1.0 +/- 0.1 TMRTG = 1.5 +/- 0.1
MA = 14.9 +/- 1.1 TGG = 95.0 +/- 8.3



Thrombin control

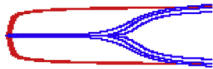
SP = 0.3 +/- 0.1 MRTG = 3.0 +/- 0.2
R = 0.5 +/- 0.1 TMRTG = 0.9 +/- 0.1
MA = 13.2 +/- 1.2 TGG = 82.1 +/- 9.6



FACTOR Xa VENOMS

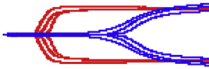
Cryptophis nigrescens

SP = 0.5 +/- 0.2 MRTG = 4.7 +/- 0.1
R = 0.6 +/- 0.2 TMRTG = 1.1 +/- 0.2
MA = 13.0 +/- 0.4 TGG = 81.0 +/- 3.1



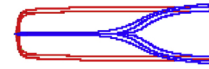
Demansia vestigiata

SP = 5.0 +/- 0.9 MRTG = 2.9 +/- 0.2
R = 5.7 +/- 0.9 TMRTG = 6.4 +/- 0.8
MA = 13.2 +/- 1.0 TGG = 76.4 +/- 5.8



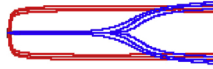
Hemiaspis signata

SP = 0.4 +/- 0.1 MRTG = 5.1 +/- 0.6
R = 0.5 +/- 0.1 TMRTG = 1.0 +/- 0.1
MA = 11.4 +/- 5.1 TGG = 62.3 +/- 8.0



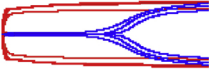
Hoplocephalus bungaroides

SP = 0.2 +/- 0.0 MRTG = 5.3 +/- 0.2
R = 0.2 +/- 0.1 TMRTG = 0.6 +/- 0.2
MA = 12.0 +/- 1.2 TGG = 63.1 +/- 7.3



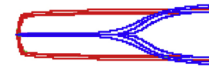
Notechis scutatus

SP = 0.2 +/- 0.0 MRTG = 7.9 +/- 1.8
R = 0.2 +/- 0.0 TMRTG = 0.3 +/- 0.0
MA = 13.0 +/- 1.7 TGG = 79.9 +/- 12.4



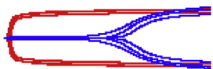
Paroplocephalus atriceps

SP = 0.4 +/- 0.1 MRTG = 4.6 +/- 0.5
R = 0.5 +/- 0.1 TMRTG = 1.0 +/- 0.1
MA = 10.8 +/- 1.1 TGG = 61.0 +/- 5.8



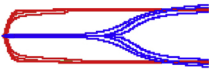
Pseudechis porphyriacus

SP = 0.7 +/- 0.1 MRTG = 4.8 +/- 0.4
R = 0.9 +/- 0.1 TMRTG = 1.3 +/- 0.2
MA = 12.5 +/- 0.8 TGG = 80.3 +/- 5.5



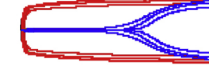
Suta punctata

SP = 0.5 +/- 0.1 MRTG = 4.3 +/- 0.7
R = 0.7 +/- 0.1 TMRTG = 1.2 +/- 0.1
MA = 12.4 +/- 1.0 TGG = 75.5 +/- 2.2



Tropidechis carinatus

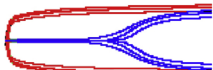
SP = 0.2 +/- 0.0 MRTG = 6.2 +/- 1.5
R = 0.2 +/- 0.1 TMRTG = 0.5 +/- 0.3
MA = 12.9 +/- 1.6 TGG = 81.4 +/- 10.3



FACTOR Xa:FACTOR Va VENOMS

Oxyuranus scutellatus

SP = 0.2 +/- 0.0 MRTG = 5.1 +/- 0.7
R = 0.3 +/- 0.1 TMRTG = 0.8 +/- 0.1
MA = 15.1 +/- 1.4 TGG = 94.3 +/- 10.9



Pseudonaja textilis

SP = 0.2 +/- 0.0 MRTG = 7.3 +/- 0.8
R = 0.2 +/- 0.0 TMRTG = 0.3 +/- 0.0
MA = 15.1 +/- 1.2 TGG = 94.6 +/- 7.2

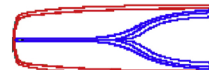


Fig. 4. Overlaid thromboelastography traces (N = 3) of 20 µg/ml venom (red) on spontaneous clotting control of human plasma (blue) for 30 min, compared to Bovine FXa and thrombin positive controls (green). Vertically narrower traces indicate weaker clots; wider traces indicate stronger clots. Values are N = 3 mean ± SD.

clade (Zdenek et al., 2019), the selection pressures guiding these biochemical derivations remains unclear and should be the subject of future work, such as examining if relative calcium dependence is a feature in differential activity upon the plasma of different prey types.

Regardless of the selection pressures resulting in the differential dependence on calcium as a biochemical cofactor, it is clear that lessened calcium dependence is a derived condition, as endogenous FXa was highly dependent upon calcium (reaching machine maximum reading time of 999 s in the absence of calcium), as were *Cryptophis*, *Demansia*, *Hemiaspis*, *P. porphyriacus*, and *Suta* venoms. The stronger potency noted for *H. signata* in this study is in contrast with a weaker result obtained in a previous study (Pycroft et al., 2012), which may be explained by neither calcium or phospholipid being included in the protocol of the previous study. The extreme variation in relative

dependence upon calcium revealed that the current grouping of prothrombin activating toxins based upon their binary cofactor dependence (Kini et al., 2001; Kini, 2005; Rosing and Tans, 1992) does not capture the biochemical variation that exists. Similarly, the relative dependence upon phospholipid also varied significantly but again without a correlation with relative speed of venom action.

There was no correlation observed between venoms best neutralised by the antivenom and relative dependency upon calcium. The venom used in the antivenom production (*N. scutatus*) exhibited lowered levels of calcium dependence compared to other members within its clade (*Hoplocephalus*, *Notechis*, *Paroplocephalus*, and *Tropidechis* genera). While *P. porphyriacus* was very well neutralised, it was very calcium dependent. Other venoms which were calcium dependent were poorly neutralised (except *S. suta*). This suggests that the molecular surface

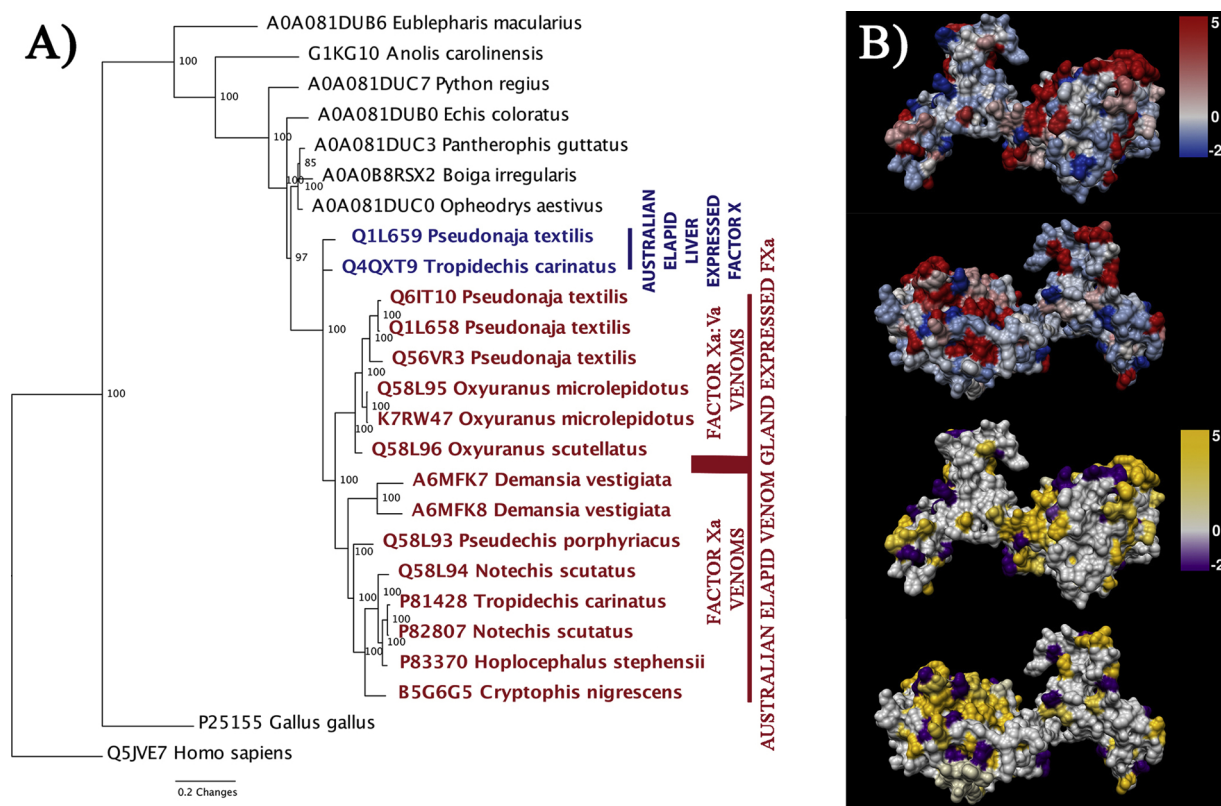


Fig. 5. Analysis of Factor X sequences. A) phylogenetic reconstruction of the toxin molecular evolutionary history including gene duplication, recruitment as a toxin, and further duplication of the gene in Australian elapids (liver-expressed FX in blue, venom FXa in red) B) the clade of toxins from genera that does not include *Oxyuranus* and *Pseudonaja* were analysed using the site-specific selection analyses FUBAR (blue and red) and MEME (purple and yellow); the results are displayed on protein structures predicted by the Phyre2 webserver.

sites involved in relative calcium dependence are not key antivenom binding sites for antibodies resulting from immunisation using *N. scutatus* venom. It is important to note that *N. scutatus* is the only FXa-rich venom used in the immunising process for Australian antivenom production. Thus, regardless of prior exposure of the horses to other Australian venoms, any antibodies present in Tiger Snake Antivenom or Polyvalent Antivenom that cross-react with FXa toxins are due to *N. scutatus* venoms. The antibodies stimulated by FXa:FVa containing *Oxyuranus* or *Pseudonaja* venoms do not cross react with each other (Zdenek et al., 2019), let alone FXa toxins from more distantly related snakes. Therefore, only Tiger Snake Antivenom (or the *N. scutatus* FXa stimulated antibodies in Polyvalent Antivenom) will cross-react with FXa toxins contained in procoagulant venoms. This explains, for example, why Black Snake Antivenom does not cross-react with *P. porphyriacus* venom, despite the fact that a venom from the same genus *Pseudechis australis* used in the antivenom production. This lack of cross-reactivity is due to *P. australis* venom lacking FXa toxins, unlike *P. porphyriacus* venom which contains them (Goldenberg et al., 2018). Thus, the only effective treatment for FXa-rich procoagulant snake venoms is either Tiger Snake Antivenom or Polyvalent Antivenom which contains antibodies raised against *N. scutatus* FXa.

Thromboelastography confirmed the generation of endogenous thrombin resulting in strong, stable fibrin clots, even for slower acting species such as *Demansia* (Fig. 2). The variation in *Demansia* speed of action was, however, correlated with variations in the relative truncation of the activation peptide sequence (Fig. 6). However, other sequence variations, such as insertions (Fig. 6), did not correlated with relative speed of action (Figs. 1 and 2). Therefore, the selection pressures for these sequence variations remain to be elucidated, with potential key variables including differential taxon-specific action, as has been noted for other genera such as *Bothrops* (Sousa et al., 2018).

In summary, this study revealed for the first time that additional lineages of Australian elapid snakes possess venoms which are potentially procoagulant and therefore may be capable of producing the same life-threatening coagulopathic effects seen clinically for more well-studied species. We also showed that, despite the ~25 million years of separation between these species and the species used in antivenom production (*N. scutatus*), the antivenom displayed an unparalleled level of cross-reactivity. However, there were substantial variations in the ability of the antivenom to neutralise venoms and thus the amount of antivenom needed may vary for equivalent doses of venom for *Cryptophis*, *Demansia*, and *Hemiaspis* venoms. The species newly documented in this study to have potent actions upon the blood have historically been involved in few, if any, snakebites due to their remote distribution or nocturnal behaviour. However, both climate change (which alters the distribution and activity periods of species), and/or continued urbanisation in Australia (which alters the distribution of humans), combined with increasing popularity in the pet trade, may lead to more envenomations by these species (Fry, 2018). Thus, our results provide important information to clinicians for the design of management strategies in the event of snakebite by such lesser known Australian elapid snake species and supports the current broad use of Tiger Snake Antivenom for FXa toxin driven procoagulant Australian snake venoms. The results of this study therefore have immediate, real-world applications for treatment of the envenomed patient. Of particular importance was that the relative effectiveness of the antivenom was not congruent with organismal relatedness, thereby reinforcing the paradigm that since venom evolves at an accelerated rate, organismal phylogeny is a poor predictor of antivenom cross-reactivity.

| Positions 181–240 | 123456789012345678901234567890123456789012345678901234567890 |
|--|---|
| Q1L659 <i>Pseudonaja textilis</i> | KTRNKREANLPDFQDFSDDYDEIDENNFVETPTNFSGLVLTQVQSNATLLKKSNDPSPD |
| Q4QXT9 <i>Tropidechis carinatus</i> | KARNKREASLPDFQDFSDDYDAIDENNFVETPTNFSGLVPTVQVQSNATLLKKSNDPSPD |
| B5G6G5 <i>Cryptophis nigrescens</i> | KARNKREASLPDFV-----VQSQATLLKKSNDPSPD |
| A6MFK8 <i>Demansia vestigiata</i> | KSRNKREASLPDFH--FSDDYDAIDENNLVET-----VQSQATLLKKSNDPSPD |
| A6MFK7 <i>Demansia vestigiata</i> | KSRNKREASLPDFQDFSDDYDAIDENNLVET-----VQSQATLLKKSNDPSPD |
| P83370 <i>Hoplocephalus stephensi</i> | KARNKREASLPDFV-----VQSQATLLKKSNDPSPD |
| P82807 <i>Notechis scutatus</i> | KARNKREASLPDFV-----VQSQATLLKKSNDPSPD |
| Q58L94 <i>Notechis scutatus</i> | KARNKREASLPDFV-----VQSQATLLKKSNDPSPD |
| Q58L95 <i>Oxyuranus microlepidotus</i> | KTRNKREASLPDFV-----VQSQATLLKKSNDPSPD |
| K7RW47 <i>Oxyuranus microlepidotus</i> | KTRNKREASLPDFV-----VQSQATLLKKSNDPSPD |
| Q58L96 <i>Oxyuranus scutellatus</i> | KTRNKREASLPDFV-----VQSQATLLKKSNDPSPD |
| Q58L93 <i>Pseudechis porphyriacus</i> | KARNKREASLPDFV-----VQSQATLLKKSNDPSPD |
| Q6IT10 <i>Pseudonaja textilis</i> | KTRNKREANLPDFV-----VQSQATLLKKSNDPSPD |
| Q1L658 <i>Pseudonaja textilis</i> | KTRNKREANLPDFV-----VQSQATLLKKSNDPSPD |
| Q56VR3 <i>Pseudonaja textilis</i> | KTRNKREASLPDFV-----VQSHNATLLKKSNDPSPD |
| P81428 <i>Tropidechis carinatus</i> | KARNKREASLPDFV-----VQSQATLLKKSNDPSPD |
| | |
| Positions 301 – 360 | 123456789012345678901234567890123456789012345678901234567890 |
| Q1L659 <i>Pseudonaja textilis</i> | ISSKK-TGRLHSVDKIYVHKQFVPA-----TYDYDIAIQLKTPIQFSENVV |
| Q4QXT9 <i>Tropidechis carinatus</i> | ISRKK-TGRLLSVDKIYVHKQFVPS-----TYDYDIAIQLKTPIQFSENVV |
| B5G6G5 <i>Cryptophis nigrescens</i> | ISRKE-TIRLLPVDKIVYVHTKQFVPSYLYG-HQNVDRKTYDYDIAIIRMKTPIQFSENVV |
| A6MFK8 <i>Demansia vestigiata</i> | ISRKE-TRHLLHVDKAYMHSKYVRA-----TYDHDIAILRLRTPIQFSENVV |
| A6MFK7 <i>Demansia vestigiata</i> | ISRKE-TRRLSVDKIYVHTKQFVPSYLYG-HQNVDRKTYDYDIAIIRMKTPIQFSENVV |
| P83370 <i>Hoplocephalus stephensi</i> | ISRKE-TRRLSVDKIYVHTKQFVPSYLYG-HQNVDRKTYDYDIAIIRMKTPIQFSENVV |
| P82807 <i>Notechis scutatus</i> | ISRKE-TRRLSVDKIYVHTKQFVPSYLYG-HQNVDRKTYDYDIAIIRMKTPIQFSENVV |
| Q58L94 <i>Notechis scutatus</i> | ISRKE-TRRLSVDKIYVHTKQFVPSYLYG-HQNVDRKTYDYDIAIIRMKTPIQFSENVV |
| K7RW47 <i>Oxyuranus microlepidotus</i> | KSRVE-TGHLLSVDKIYVHKQFVPPKKGKGYEFYKFDLVSVDYDIAIIRMKTPIQFSENVV |
| Q58L96 <i>Oxyuranus scutellatus</i> | ISRKN-PGRLLSVDKIYVHKQFVPPKKGKGYEFYKFDLVSVDYDIAIIRMKTPIQFSENVV |
| Q58L95 <i>Oxyuranus microlepidotus</i> | KSRVE-TGHLLSVDKIYVHKQFVPPKKGKGYEFYKFDLVSVDYDIAIIRMKTPIQFSENVV |
| Q58L93 <i>Pseudechis porphyriacus</i> | ISRKE-TRHLLSVDKAYVHTKQFVLA-----TYDYDIAIQLKTPIQFSENVV |
| Q6IT10 <i>Pseudonaja textilis</i> | KSRVE-TGHLLSVDKIYVHKQFVPPKQKAY---KFDLAAVDYDIAIIRMKTPIQFSENVV |
| Q1L658 <i>Pseudonaja textilis</i> | KSRVE-TGHLLSVDKIYVHKQFVPPKQKAY---KFDLAAVDYDIAIIRMKTPIQFSENVV |
| Q56VR3 <i>Pseudonaja textilis</i> | RSRAE-TGPLLSVDKIYVHKQFVPPKKSQEFYKFDLVSVDYDIAIIRMKTPIQFSENVV |
| P81428 <i>Tropidechis carinatus</i> | ISRKE-TRRLSVDKIYVHTKQFVPPNYYV-HQNVDRKTYDYDIAIIRMKTPIQFSENVV |

Fig. 6. Sequences alignment comparing the endogenous Factor X form secreted in the liver (blue) relative to the Factor Xa forms specifically secreted in the venom gland (red). In positions 195–223, the activation peptide has been deleted in the venom forms except for in the most basal species (*Demansia vestigiata*), which is only partially truncated. Insertions (function unknown) are present in the venom gland forms of some species in the alignment positions 326–338. Only alignment positions relative to these insertions/deletions are shown; the full length sequence alignments are not presented here.

Transparency document

The [Transparency document](#) associated with this article can be found in the online version.

Declaration of Competing Interest

The authors declare no conflict of interest.

Acknowledgments

CNZ, BODB, and DD were recipients of PhD scholarships administered by the University of Queensland. BGF was funded by University of Queensland Major Infrastructure and Equipment grant 2016000654, UQ Science with Impact grant, and ARC Discovery Project grant DP190100304.

Appendix A. Supplementary data

Supplementary material related to this article can be found, in the online version, at doi:<https://doi.org/10.1016/j.toxlet.2019.08.014>.

References

Brust, A., Sunagar, K., Undheim, E.A.B., Vetter, I., Yang, D.C., Casewell, N.R., Jackson, T.N.W., Koludarov, I., Alewood, P.F., Hodgson, W.C., Lewis, R.J., King, G.F., Antunes, A., Hendrikx, I., Fry, B.G., 2012. Differential evolution and neofunctionalization of snake venom metalloprotease domains. *Mol. Cell Proteomics* 12, 651–663. <https://doi.org/10.1074/mcp.m112.023135>.

Chatrath, S.T., Chapeaurouge, A., Lin, Q., Lim, T.K., Dunstan, N., Mirtschin, P., Kumar, P.P., Kini, R.M., 2010. Identification of novel proteins from the venom of a cryptic snake *Drysdalia coronoides* by a combined transcriptomics and proteomics approach. *J. Proteome Res.* 10, 739–750. <https://doi.org/10.1021/pr1008916>.

Cipriani, V., Debono, J., Goldenberg, J., Jackson, T.N.W., Arbuckle, K., Dobson, J., Koludarov, I., Li, B., Hay, C., Dunstan, N., Allen, L., Hendrikx, I., Fai, H., Fry, B.G., 2017. Correlation between ontogenetic dietary shifts and venom variation in Australian brown snakes (*Pseudonaja*). *Comp. Biochem. Physiol. Part C* 197, 53–60. <https://doi.org/10.1016/j.cbpc.2017.04.007>.

Colman, R., Clowes, A., George, J., Goldhaber, S., Marder, V., 2006. Overview of hemostasis. In: Colman, R., Marder, V., Clowes, A., George, J., Goldhaber, S. (Eds.), *Hemostasis and Thrombosis: Basic Principles and Clinical Practice*. Lippincott Williams & Wilkins, Philadelphia, PA, USA, pp. 3–16.

Consortium, T.U., 2017. UniProt: the universal protein knowledgebase. *Nucleic Acids Res.* 45, D158–D169. <https://doi.org/10.1093/nar/gkw1099>.

Dashevsky, D., Fry, B., 2018. Ancient diversification of three-finger toxins in *Micrurus* coral snakes. *J. Mol. Evol.* 86, 58–67. <https://doi.org/10.1007/s00239-017-9825-5>.

Edgar, R.C., 2004. MUSCLE: multiple sequence alignment with high accuracy and high throughput. *Nucleic Acids Res.* 32, 1792–1797. <https://doi.org/10.1093/nar/gkh340>.

Fry, B.G., 2005. From genome to "venome": molecular origin and evolution of the snake venom proteome inferred from phylogenetic analysis of toxin sequences and related body proteins. *Genome Res.* 15 (March 3), 403–420 2005.

Fry, B.G., 2018. Snakebite: when the human touch becomes a bad touch. *Toxins (Basel)* 10, 1–24. <https://doi.org/10.3390/toxins10040170>.

Fry, B.G., 1999. Structure-function properties of venom components from Australian elapids. *Toxicon* 37, 11–32. [https://doi.org/10.1016/S0041-0101\(98\)00125-1](https://doi.org/10.1016/S0041-0101(98)00125-1).

Fry, B.G., Scheib, H., van der Weerd, L., Young, B., McNaughtan, J., Ramjan, S.F.R., Vidal, N., Poelmann, R.E., Norman, J.A., 2008. Evolution of an arsenal: structural and functional diversification of the venom system in the advanced snakes (Caenophidia). *Mol. Cell Proteomics* 7, 215–246. <https://doi.org/10.1074/mcp.M700094-MCP200>.

Gan, M., O'Leary, M., Brown, S., Jacoby, T., Tankel, A., Gavaghan, C., Garrett, P., Isbister, G., 2009. Envenoming by the rough-scaled snake (*Tropidechis carinatus*): a series of confirmed cases. *Med. J. Aust.* 191, 183–186.

Goldenberg, J., Cipriani, V., Jackson, T.N.W., Arbuckle, K., Debono, J., Dashevsky, D., Panagides, N., Ikononopoulou, M.P., Koludarov, I., Li, B., Santana, R.C., Nouwens, A., Jones, A., Hay, C., Dunstan, N., Allen, L., Bush, B., Miles, J.J., Ge, L., Kwok, H.F., Fry, B.G., 2018. Proteomic and functional variation within black snake venoms (Elapidae: *pseudechis*) jonathan. *Comp. Biochem. Physiol. Part C* 205, 53–61.

Greenberg, D., Davie, E., 2006. The blood coagulation factors: their complementary DNAs, genes, and expression. In: Colman, R., Marder, V., Clowes, A., George, J., Goldhaber, S. (Eds.), *Thrombosis and Haemostasis: Basic Principles and Clinical Practice*. Lippincott Williams & Wilkins, Philadelphia, PA, USA, pp. 21–57.

Gulati, A., Isbister, G.K., Duffull, S.B., 2013. Effect of Australian elapid venoms on blood coagulation: australian Snakebite Project (ASP-17). *Toxicon* 61, 94–104. <https://doi.org/10.1016/j.toxicon.2013.05.014>.

- org/10.1016/j.toxicon.2012.11.001.
- Isbister, G.K., 2010. Snakebite doesn't cause disseminated intravascular coagulation: coagulopathy and thrombotic microangiopathy in snake envenoming. *Semin. Thromb. Hemost.* 36, 444–451.
- Isbister, G.K., Brown, S.G., MacDonald, E., White, J., Currie, B.J., 2008. Current use of Australian snake antivenoms and frequency of immediate-type hypersensitivity reactions and anaphylaxis. *Med. J. Aust.* 188, 473–476 <https://doi.org/10.1016/j.mja.2007.11.011>.
- Isbister, G.K., Duffull, S.B., Brown, S.G.A., 2009. Failure of antivenom to improve recovery in Australian snakebite coagulopathy. *Q. J. Med.* 102, 563–568. <https://doi.org/10.1093/qjmed/hcp081>.
- Jackson, T.N.W., Sunagar, K., Undheim, E.A.B., Koludarov, I., Chan, A.H.C., Sanders, K., Ali, S.A., Hendrikx, I., Dunstan, N., Fry, B.G., 2013. Venom down under: dynamic evolution of Australian elapid snake. *Toxins* 5, 2621–2655. <https://doi.org/10.3390/toxins5122621>.
- Jiang, Y., Li, Y., Lee, W., Xu, X., Zhang, Yue, Zhao, R., Zhang, Yun, Wang, W., 2011. Venom gland transcriptomes of two elapid snakes (*Bungarus multicinctus* and *Naja atra*) and evolution of toxin genes. *BMC Genomics* 12, 1–13. <https://doi.org/10.1186/1471-2164-12-1>.
- Joseph, J.S., Chung, M.C., Jeyaseelan, K., Kini, R.M., 1999. Amino acid sequence of trocristan, a prothrombin activator from *Tropidochis carinatus* venom: its structural similarity to coagulation factor Xa. *Blood* 94, 621–631. [https://doi.org/10.1016/S0001-0101\(01\)00218-5](https://doi.org/10.1016/S0001-0101(01)00218-5).
- Juárez, P., Comas, I., González-Candelas, F., Calvete, J.J., 2008. Evolution of snake venom disintegrins by positive Darwinian selection. *Mol. Biol. Evol.* 25, 2391–2407. <https://doi.org/10.1093/molbev/msn179>.
- Kasturiratne, A., Wickremasinghe, A.R., Silva, N.D., Gunawardena, N.K., 2008. The global burden of snakebite: a literature analysis and modelling based on regional estimates of envenoming and deaths. *PLoS Med.* 5, 1591–1604. <https://doi.org/10.1371/journal.pmed.0050218>.
- Kelley, L.A., Mezulis, S., Yates, C., Wass, M., Sternberg, M., 2015. The Pyre2 web portal for protein modelling, prediction, and analysis. *Nat. Protoc.* 10, 845–858. <https://doi.org/10.1038/nprot.2015-053>.
- Kini, M., Morita, T., Rosing, J., 2001. Classification and nomenclature of prothrombin activators isolated from snake venoms. *Thromb. Hemost.* 85, 710–711.
- Kini, R.M., 2005. The intriguing world of prothrombin activators from snake venom. *Toxicon* 45, 1133–1145. <https://doi.org/10.1016/j.toxicon.2005.02.019>.
- Kini, R.M., Rao, V.S., Joseph, J.S., 2002. Procoagulant proteins from snake venoms. *Haemostasis* 31, 218–224 <https://doi.org/10.1007/s00011-002-0018-5>.
- Kwong, S., Kini, R., 2011. Duplication of coagulation factor genes and evolution of snake venom prothrombin activators. In: Friedberg, F. (Ed.), *Gene Duplication*. InTechOpen.com.
- Lane, J., O'Leary, M.A., Isbister, G.K., 2011. Coagulant effects of black snake (*Pseudechis* spp.) venoms and in vitro efficacy of commercial antivenom. *Toxicon* 58, 239–246. <https://doi.org/10.1016/j.toxicon.2011.05.020>.
- Larsson, A., 2014. AliView: a fast and lightweight alignment viewer and editor for large datasets. *Bioinformatics* 30, 3276–3278. <https://doi.org/10.1093/bioinformatics/btu531>.
- Lavin, M.F., Masci, P.P., 2009. Prothrombinase complexes with different physiological roles. *Thromb. Haemost.* 102, 421–423. <https://doi.org/10.1160/TH09-08-0050>.
- Lee, M.S.Y., Sanders, K.L., King, B., Palci, A., 2016. Diversification rates and phenotypic evolution in venomous snakes (Elapidae). *R. Soc. Open Sci.* 3, 1–11. <https://doi.org/10.5061/dryad.cr788>.
- Lister, C., Arbuckle, K., Jackson, T.N.W., Debono, J., Zdenek, C.N., Dashevsky, D., Dunstan, N., Allen, L., Hay, C., Bush, B., Gillett, A., Fry, B.G., 2017. Catch a tiger snake by its tail: differential toxicity, co-factor dependence and antivenom efficacy in a procoagulant clade of Australian venomous snakes. *Comp. Biochem. Physiol. Part C* 202, 39–54. <https://doi.org/10.1016/j.cbpc.2017.07.005>.
- McCleary, R.J.R., Sridharan, S., Dunstan, N.L., Mirtschin, P.J., Kini, R.M., 2016. Proteomic comparisons of venoms of long-term captive and recently wild-caught Eastern brown snakes (*Pseudonaja textilis*) indicate venom does not change due to captivity. *J. Proteomics* 144, 51–62. <https://doi.org/10.1016/j.jprot.2016.05.027>.
- Mirtschin, P.J., Dunstan, N., Hough, B., Hamilton, E., Klein, S., Lucas, J., Millar, D., Madaras, F., Nias, T., 2006. Venom yields from Australian and some other species of snakes. *Ecotoxicology* 15, 531–538. <https://doi.org/10.1007/s10646-006-0089-x>.
- Murrell, B., Moola, S., Mabona, A., Weighill, T., Sheward, D., Kosakovsky Pond, S.L., Scheffler, K., 2013. FUBAR: a fast, unconstrained Bayesian Approximation for inferring selection. *Mol. Biol. Evol.* 30, 1196–1205. <https://doi.org/10.1093/molbev/mst030>.
- Murrell, B., Wertheim, J.O., Moola, S., Weighill, T., Scheffler, K., Kosakovsky Pond, S.L., 2012. Detecting individual sites subject to episodic diversifying selection. *PLoS Genet.* 8. <https://doi.org/10.1371/journal.pgen.1002764>.
- O'Leary, M.A., Kornhauser, R.S., Hodgson, W.C., Isbister, G.K., 2009. An examination of the activity of expired and mistreated commercial Australian antivenoms. *Trans. R. Soc. Trop. Med. Hyg.* 103, 937–942. <https://doi.org/10.1016/j.trstmh.2008.11.011>.
- Ouilon, B., Dobson, J.S., Zdenek, C.N., Arbuckle, K., Lister, C., Coimbra, F.C.P., op den Brouw, B., Debono, J., Rogalski, A., Violette, A., Fourmy, R., Frank, N., Fry, B.G., 2018. Factor X activating *Atractaspis* snake venoms and the relative coagulotoxicity neutralising efficacy of African antivenoms. *Toxicol. Lett.* 288. <https://doi.org/10.1016/j.toxlet.2018.02.020>.
- Paradis, E., Claude, J., Strimmer, K., 2004. APE: Analyses of phylogenetics and evolution in R language APE. *Bioinformatics* 20, 289–290. <https://doi.org/10.1093/bioinformatics/btg412>.
- Petersen, E.F., Goddard, T.D., Huang, C.C., Couch, G.S., Greenblatt, D.M., Meng, E.C., Ferrin, T.E., 2004. UCSF Chimera—a visualization system for exploratory research and analysis. *J. Comput. Chem.* 25, 1605–1612. <https://doi.org/10.1002/jcc.20084>.
- Pond, S.L.K., Frost, S.D.W., Muse, S.V., 2005. HyPhy: hypothesis testing using phylogenies. *Bioinformatics* 21, 676–679. <https://doi.org/10.1093/bioinformatics/bti079>.
- Pycroft, K., Fry, B.G., Isbister, G.K., Kuruppu, S., Lawrence, J., Ian Smith, A., Hodgson, W.C., 2012. Toxicology of venoms from five Australian lesser known elapid snakes. *Basic Clin. Pharmacol. Toxicol.* 111 (4), 268–274. <https://doi.org/10.1111/j.1742-7843.2012.00907>.
- Rao, V.S., Kini, R.M., 2002. Pseutarin C, a prothrombin activator from *Pseudonaja textilis* venom: its structural and functional similarity to mammalian coagulation factor Xa-Va complex. *Thromb. Hemost.* 88, 611–619.
- Rao, V.S., Swarup, S., Kini, R.M., 2004. The catalytic subunit of pseutarin C, a group C prothrombin activator from the venom of *Pseudonaja textilis*, is structurally similar to mammalian blood coagulation factor Xa. *Thromb. Haemost.* 92, 509–521. <https://doi.org/10.1160/TH04-03-0144>.
- Revell, L.J., 2012. phytools: An R package for phylogenetic comparative biology (and other things). *Methods Ecol. Evol.* 3, 217–223. <https://doi.org/10.1111/j.2041-210X.2011.00169.x>.
- Reza, M., Swarup, S., Kini, R.M., 2005. Two parallel prothrombin activator systems in Australian rough-scaled snake, *Tropidochis carinatus*: structural comparison of venom prothrombin activator with blood coagulation factor X. *Thromb. Haemost.* 93, 40–47. <https://doi.org/10.1160/TH04-07-0435>.
- Reza, M.A., Le, T.N.M., Swarup, S., Kini, R.M., 2006. Molecular evolution caught in action: gene duplication and evolution of molecular isoforms of prothrombin activators in *Pseudonaja textilis* (brown snake). *J. Thromb. Haemost.* 4, 1346–1353. <https://doi.org/10.1111/j.1538-7836.2006.01969.x>.
- Rogalski, A., Soerensen, C., op den Brouw, B., Lister, C., Dashvesky, D., Arbuckle, K., Gloria, A., Zdenek, C.N., Casewell, N.R., Gutiérrez, J.M., Wüster, W., Ali, S.A., Masci, P., Rowley, P., Frank, N., Fry, B.G., 2017. Differential procoagulant effects of saw-scaled viper (Serpentes: viperidae: *echis*) snake venoms on human plasma and the narrow taxonomic ranges of antivenom efficacies. *Toxicol. Lett.* 280, 159–170. <https://doi.org/10.1016/j.toxlet.2017.08.020>.
- Rokyta, D.R., Wray, K.P., Lemmon, A.R., Lemmon, E.M., Caudle, S.B., 2011. A high-throughput venom-gland transcriptome for the Eastern Diamondback Rattlesnake (*Crotalus adamanteus*) and evidence for pervasive positive selection across toxin classes. *Toxicon* 57, 657–671. <https://doi.org/10.1016/j.toxicon.2011.01.008>.
- Ronquist, F., Teslenko, M., Van Der Mark, P., Ayres, D.L., Darling, A., Höhna, S., Larget, B., Liu, L., Suchard, M.A., Huelsenbeck, J.P., 2012. MrBayes 3.2: efficient bayesian phylogenetic inference and model choice across a large model space. *Syst. Biol.* 61, 539–542. <https://doi.org/10.1093/sysbio/sysbio029>.
- Rosing, J., Tans, G., 1992. Structural and functional properties of snake venom prothrombin activators. *Toxicon* 30, 1515–1527. [https://doi.org/10.1016/0041-0101\(92\)90023-X](https://doi.org/10.1016/0041-0101(92)90023-X).
- Sanders, K.L., Lee, M.S.Y., Leys, R., Foster, R., Scott Keogh, J., 2008. Molecular phylogeny and divergence dates for Australasian elapids and sea snakes (hydrophiinae): evidence from seven genes for rapid evolutionary radiations. *J. Evol. Biol.* 21, 682–695. <https://doi.org/10.1111/j.1420-9101.2008.01525.x>.
- Schiermeier, Q., 2019. Snakebite crisis gets US\$100-million boost for better antivenoms: wellcome Trust launches research initiative for long-neglected health problem. *Nat. News*.
- Sousa, L., Zdenek, C.N., Dobson, J., op den Brouw, B., Coimbra, F., Gillett, A., Del-Rei, T., Chalkidiki, H., Sant'Anna, S., Teixeira-da-Rocha, M., Grego, K., Travaglia Cardoso, S., Moura da Silva, A., Fry, B., Sousa, L.F., Zdenek, C.N., Dobson, J.S., op den Brouw, B., Coimbra, F., Gillett, A., Del-Rei, T.H.M., Chalkidiki, H., de, M., Sant'Anna, S., Teixeira-da-Rocha, M.M., Grego, K., Travaglia Cardoso, S.R., Moura da Silva, A.M., Fry, B.G., 2018. Coagulotoxicity of *Bothrops* (lancehead pit-vipers) venoms from Brazil: differential biochemistry and antivenom efficacy resulting from prey-driven venom variation. *Toxins (Basel)* 10, 411. <https://doi.org/10.3390/toxins10100411>.
- St Pierre, L., Birrell, G.W., Earl, S.T., Wallis, T.P., Gorman, J.J., De Jersey, J., Masci, P.P., Lavin, M.F., 2007. Diversity of toxic components from the venom of the evolutionary distinct black whip snake, *Demansia vestigiata*. *J. Proteome Res.* 6, 3093–3107. <https://doi.org/10.1021/pr0701613>.
- Strickland, J.L., Carter, S., Kraus, F., Parkinson, C.L., 2016. Snake evolution in Melanesia: origin of the Hydrophiinae (Serpentes, Elapidae), and the evolutionary history of the enigmatic New Guinean elapid *Toxicocalamus*. *Zool. J. Linn. Soc.* 178, 663–678. <https://doi.org/10.1111/zoj.12423>.
- Sutherland, S., Tibballs, J., 2001. *Australian Animal Toxins: the Creatures, Their Toxins and Care of the Poisoned Patient*, 2nd ed. Oxford University Press, South Melbourne.
- Trabi, M., Sunagar, K., Jackson, T.N.W., Fry, B.G., 2015. Factor Xa enzymes. In: Fry, B.G. (Ed.), *Venomous Reptiles and Their Toxins: Evolution, Pathophysiology and Biodiscovery*. Oxford University Press, New York, NY, pp. 261–266.
- Tracy, P., Eide, L., Bowie, J., Mann, K., 1982. Radioimmunoassay of Factor V in human plasma and platelets. *Blood* 60, 59–63.
- White, J., 2005. Snake venoms and coagulopathy. *Toxicon* 45, 951–967. <https://doi.org/10.1016/j.toxicon.2005.02.030>.
- Youngman, N.J., Zdenek, C.N., Dobson, J.S., Bittenbinder, M.A., Gillett, A., Hamilton, B., Dunstan, N., Allen, L., Veary, A., Veary, E., Fry, B.G., 2018. Mud in the blood: novel potent anticoagulant coagulotoxicity in the venoms of the Australian elapid snake genus *Denisonia* (mud adders) and relative antivenom efficacy. *Toxicol. Lett.* 302, 1–6. <https://doi.org/10.1016/j.toxlet.2018.11.015>.
- Zdenek, C.N., Hay, C., Arbuckle, K., Jackson, T.N.W., Bos, M.H.A., op den Brouw, B., Debono, J., Allen, L., Dunstan, N., Morley, T., Herrera, M., Gutiérrez, J.M., Williams, D.J., Fry, B.G., 2019. Coagulotoxic effects by brown snake (*Pseudonaja*) and taipan (*Oxyuranus*) venoms, and the efficacy of a new antivenom. *In Vitro* 58, 97–109. <https://doi.org/10.1016/j.tiv.2019.03.031>.